Published in final edited form as:
Glia. 2011 June ; 59(6): 857–868. doi:10.1002/glia.21154.

Loss of adenomatous polyposis coli in Bergmann glia disrupts their unique architecture and leads to cell non-autonomous neurodegeneration of cerebellar Purkinje neurons

Xiaohong Wang[1], **Tetsuya Imura**[1], **Michael V. Sofroniew**[2], and **Shinji Fushiki**[1]

[1]Department of Pathology and Applied Neurobiology, Graduate School of Medical Science, Kyoto Prefectural University of Medicine, Kyoto 602-8566, Japan

[2]Department of Neurobiology, David Geffen School of Medicine, University of California, Los Angeles, Los Angeles, California 90095-1763

Abstract

The tumor suppressor adenomatous Polyposis Coli (APC) is a multifunctional protein that inhibits the Wnt/beta-catenin signaling pathway and regulates the microtubule and actin cytoskeletons. Using conditional knockout (CKO) mice in which the APC gene is inactivated in glial fibrillary acidic protein (GFAP)-expressing cells, we show a selective and critical role for APC in maintaining the morphology and function of cerebellar Bergmann glia. APC-CKO mice developed Bergmann glia normally until the accumulation of beta-catenin started around postnatal day 10 (P10). Their radial fibers then became shortened with a marked reduction of branching collaterals and their cell bodies translocated into the molecular layer followed by loss of their pial contact and transformation into stellate-shaped cells by P21. Purkinje neurons were normal in appearance and number at P21, but there was significant loss of Purkinje neurons and cerebellar atrophy by middle age. Outside the cerebellum, neither beta-catenin accumulation nor morphological changes were identified in GFAP-expressing astroglia, indicating region-specific effects of APC deletion and an essential role for APC in maintaining the unique morphology of Bergmann glia as compared with other astroglia. These results demonstrate that loss of APC selectively disrupts the Bergmann glial scaffold in late postnatal development and leads to cerebellar degeneration with loss of Purkinje neurons in adults, providing another potential mechanism for region-specific non-cell autonomous neurodegeneration.

Keywords

astrocytes; ataxia; beta-catenin; glial fibrillary acid protein; Wnt

Introduction

Bergmann glia in cerebellar cortex are a specialized type of astroglia that display a radial glial morphology. The radial processes of Bergmann glia guide the migration of granule cells during development and their endfeet form the superficial glia limitans. In addition to these radial glial features, Bergmann glia extend numerous collateral branches from their

Correspondence should be addressed to Tetsuya Imura, Department of Pathology and Applied Neurobiology, Graduate School of Medical Science, Kyoto Prefectural University of Medicine, Kawaramachi Hirokoji, Kamigyo-ku, Kyoto 602-8566, Japan, Tel: 81-75-251-5849; Fax: 81-75-251-5849; timura@koto.kpu-m.ac.jp.

Disclosure of Potential Conflicts of Interest
The authors indicate no potential conflicts of interest.

main radial fibers and these collaterals ensheath almost all synapses on Purkinje cell dendrites to regulate ionic homeostasis and synaptic activity (Grosche et al. 1999; Iino et al. 2001; Lippman et al. 2008; Yamada et al. 2000). Thus, Bergmann glia play various important roles in both the developing and adult cerebellar cortex. Consistent with this notion, the dysfunction of Bergmann glia is implicated in some neurodegenerative disorders (Custer et al. 2006; Shiwaku et al. 2010). There is compelling evidence that cell-to-cell interaction is crucial for the differentiation of Bergmann glia and several signaling pathways have been identified to regulate the process (Belvindrah et al. 2006; Eiraku et al. 2005; Lin et al. 2009). However, molecular mechanisms in maintaining such a unique morphology of this cell type remain unclear.

The tumor suppressor adenomatous polyposis coli (APC) was originally identified as a causative molecule of human familial adenomatous polyposis syndrome and a negative regulator of the canonical Wnt signaling pathway (Kinzler et al. 1991; Nishisho et al. 1991). APC induces the degradation of beta-catenin, a downstream effecter of the Wnt pathway, to prevent the nuclear translocation of beta-catenin and the activation of its target genes. Moreover, APC regulates the microtubule and actin cytoskeletons by either binding to microtubule plus ends and EB1 or modulating Rho-GTPase through Asef and IQGAP1 (Aoki and Taketo 2007; Hanson and Miller 2005; Nathke 2004). APC is particularly abundant both in the developing and adult central nervous system (CNS)(Bhat et al. 1994), and it contributes to a variety of brain functions including axon outgrowth, postsynaptic assembly, neuronal differentiation, and embryonic radial glial polarity (Ivaniutsin et al. 2009; Temburni et al. 2004; Yokota et al. 2009; Zhou et al. 2004; Imura et al. 2010). In the present study, we demonstrate that APC deletion from GFAP-expressing astroglia selectively disrupts the unique cellular architecture of Bergmann glia during the late postnatal period followed by a significant loss of Purkinje cells by middle age. APC is thus required to maintain a unique morphology of Bergmann glia and Bergmann glial scaffold is essential for the survival of Purkinje cells.

Materials and Methods

Mice

APC-CKO mice were generated as previously described (Imura et al. 2010). Briefly, mGFAP-Cre mice of line 73.12 were cross-bred with APC^{580S} mice on a C57BL/6 background to obtain mGFAP-Cre/ $APC^{580S/580S}$ (APC-CKO) mice. APC^{580S} mice in which Exon 14 of the *APC* gene is flanked by the two loxP sites was kindly provided by Dr. Tetsuo Noda, the Cancer Institute, Tokyo, Japan. Cre-mediated recombination leads to a frameshift mutation at codon 580 and generates a C-terminally truncated protein lacking the binding domains for its major partners (Shibata et al. 1997). mGFAP-Cre mice, generated using a 15 kb mouse GFAP promoter cassette (clone 445), have been shown to selectively target Cre activity in GFAP-expressing cells including astroglia and adult neural stem cells in forebrain (Garcia et al. 2004; Herrmann et al. 2008). Littermate mice carrying no mGFAP-Cre ($APC^{580S/+}$ and $APC^{580S/580S}$ mice) were used as controls unless otherwise noted. mGFAP-Cre mice were also cross-bred with the Cre enhanced green fluorescent protein (GFP) reporter mice kindly provided by Dr. Jun-ichi Miyazaki, Osaka University to monitor Cre-mediated recombination at the single cell level (Kawamoto et al. 2000). mGFAP-Cre/GFP/$APC^{580S/580S}$ mice are indicated as APC-CKO reporter mice and mGFAP-Cre/GFP/$APC^{+/+}$ mice from the same breeding colony are indicated as control mGFAP-Cre reporter mice. Mice were housed in a 12 h light/dark cycle in an SPF facility with controlled temperature and humidity and allowed *ad libitum* access to food and water, and experiments conducted according to protocols approved by the Committee for Animal Research, Kyoto Prefectural University of Medicine, Japan, and the animals were handled in

accordance with the guidelines for the Care and Use of Laboratory Animals of Kyoto Prefectural University of Medicine.

Behavioral analysis—The footprint pattern was obtained from middle-aged CKO mice and their littermate controls. After coating of hindfeet with nontoxicink, mice were allowed to walk through a tunnel (50 cm long,8 cm wide) with paper lining the floor. Motor coordination was also assessed by the bar cross test. Middle-aged CKO mice and their littermate controls were placed in the middle of a narrow bar (8 mm in width) at a height of ~40 cm above the cage floor to discourage jumping. The time each mouse can stay on the bar before falling off (maximum 60 sec) was measured.

Histological procedures—Mice were perfused transcardially with buffered 4% paraformaldehyde under deep anesthesia. The brains were removed, post-fixed, and cryoprotected in buffered 30% sucrose. Frozen sections were prepared using a cryostat microtome (Leica). In some cases, fixed tissues were embedded in paraffin and paraffin sections at 4 micrometer thickness were cut with a microtome. Primary and secondary antibodies used for immunohistochemistry were as follows; mouse anti-GFAP (Sigma, St, Louis, MO), rabbit anti-GFAP (Chemicon, Temecula, CA), mouse anti-S100beta (Abcam, Cambradge, UK), rabbit anti-S100 (Dako, Glostrup, Denmark). mouse anti-NeuN (Millipore, Billerica, MA), mouse anti-beta-catenin (BD Bioscience, Franklin, Lakes, NJ), rabbit anti-beta-catenin (Sigma), mouse anti-parvalbumin (Swant, Bellinzona, Switzerland), rabbit anti-caspase-3 (ASP175) (Cell signaling, Beverly, MA), rabbit anti-BLBP (Abcam), rat anti-GFP (Nacalai, Osaka, Japan), rabbit anti-GFP (Invitrogen, Carlsbad, CA), mouse anti-nestin (Chemicon), mouse anti-calbindin D-28 (Swant), rabbit anti-laminin (Abcam), rabbit anti-Iba1 (Wako, Osaka, Japan), mouse anti-CD31 (BD Bioscience). Fluorescence immunohistochemistry was performed using AlexaFluor tagged secondary antibodies Alexa 488, Alexa 568, or Alexa 633 (Invitrogen). Nuclei were counterstained with either 4′,6-diamidino-2-phenylindole (DAPI; Invitrogen) or TOPRO-3 (Invitrogen). Bright-field immunohistochemistry was performed using Histofine Simplestain Max-PO (Nichirei), and diaminobenzidine (Sigma) as the developing agents. Stained sections were examined and photographed using bright-field and fluorescence microscopy (Olympus), and scanning confocal laser microscopy (FV1000; Olympus). Stacks of 0.5-μm or 0.8-μm-thick optical slices were collected through the z axis of tissue sections of regions to be analyzed.

Morphometric and statistical evaluation

For quantification of S100-positive cells in the Purkinje cell layer (PCL) and molecular layer (MOL), three sagittal cerebellar sections (4 μm thickness) at identical levels (approximately 200 μm apart) per mouse were selected and the three counting frames (500 μm in lateral diameter) containing the entire PCL and MOL were applied within lobules III, V, VIII on each section. Purkinje neurons were easily identified and the PCL was defined as the region from 5 μm below the bottom to 10 μm above the top of Purkinje cell somata. The number of S100-positive cells was separately counted in the PCL and MOL, and expressed as cells per cm PCL. For quantification of Purkinje neurons, three Nissl-stained sagittal cerebellar sections (4 μm thickness) at identical levels (approximately 200 μm apart) per mouse were selected and the total number of Purkinje cells was counted and expressed as cells per section. The number of caspase-3-positive cells was counted in the same way as described above and expressed as cells per section. For the proportion of GFP-positive neurons in the granule cell layer, more than 500 NeuN-positive neurons from more than three independent regions were evaluated per mice and the percentage of NeuN-positive cells that were also GFP-positive as determined by confocal analysis. Values were shown as the mean + SD and statistical evaluations were performed using Prism software (GraphPad).

Quantitative RT-PCR

Total RNA was isolated from each sample using an RNeasy extraction kit with a DNase I treatment (Qiagen) and cDNA was synthesized from 2 μg of total RNA by SuperScript II reverse transcriptase (Invitrogen). Quantitative real-time polymerase chain reaction (PCR) using the Sybr Green I reagent (Takara) was performed with ABI7000 (Applied Biosystems). The gene-specific primer used for Axin2 [NM_015732;] was; Forward; 5′-CACTTTGGCACAGCTAGAGG-3′, Reverse; 5′-TGCCTGACCAGCAGCCGAGT-3′. Control experiments were performed without reverse transcriptase to ensure that the results were not due to amplifications of genomic DNA. PCR product identity was confirmed by electrophoresis and by melting-point analysis. The expression value of each gene was normalized to the amount of glyceraldehyde-3-phosphate dehydrogenase (GAPDH) gene and a relative amount of transcript was calculated compared with control samples.

Results

APC CKO mice exhibited ataxia and cerebellar atrophy by middle age (6 months)

We have previously generated mGFAP-Cre/ $Apc^{580S/580S}$ (APC-CKO) mice and have identified impaired neurogenesis from GFAP-expressing postnatal and adult neural stem cells that generate restricted sub-populations of neurons in the hippocampus and olfactory bulb. APC-CKO mice also variably exhibited gut and ocular abnormalities due to APC deletion from GFAP-expressing enteric glia and lens epithelium, which made a detailed behavioral analysis difficult in these mice (Imura et al. 2010). Nevertheless, we noticed that an abnormal gait became apparent in APC-CKO mice by middle age, postnatal day (P) 180. They displayed a wide-based gait with occasional falling. The footprint patterns of CKO mice showed a poorly coordinated dragged gait (Fig. 1A). In addition, APC-CKO mice fell off the narrow bar significantly earlier than littermate controls (26.8+18.2 sec and 52.3+12.3 sec in CKO and control mice, respectively. n=4–6, $p<0.05$, *t* test). APC-CKO mice thus exhibited signs of ataxia, which led us to investigate whether cerebellar abnormalities are induced by APC deletion.

Macroscopically the cerebella of juvenile (P21) and young adult (P56) APC-CKO mice were indistinguishable from those of littermate controls (*data not shown*), whereas in middle-aged CKO mice the cerebella were visibly smaller (Fig. 1B). Nissl staining showed that the cerebellar cytoarchitecture of juvenile (P21) and young adult (P56) CKO mice was indistinguishable from that of littermates (Fig. 1C) and revealed pronounced atrophy and degenerative changes in the cerebellar cortex of middle aged (P180) CKO mice (F*ig. 1C*). Degenerative changes were particularly severe in lobules VI, VII, and VIII, where the thickness of the molecular layer was markedly decreased (Fig. 1D).

Together, these findings suggest that the basic development of the cerebellar cortex is preserved in APC-CKO mice and that the pronounced atrophy and degeneration that are present at middle age occur primarily after development.

mGFAP-Cre (line 73.12) targeted Bergmann glia and astrocytes but not Purkinje neurons in the cerebellar cortex

To investigate the mechanisms of cerebellar atrophy in APC-CKO mice, we first identified at the single cell level, those cell types in which Cre-mediated recombination occurred in the cerebellar cortex using control mGFAP-Cre-reporter mice (Fig 2A–F). In the Purkinje cell layer, the reporter GFP was expressed exclusively in cells with small somata that extended radial fibers toward the pial surface with numerous collateral branches (Fig. 2A). All of these cells were positive for the astroglial markers GFAP and S100 (Fig. 2B, C) demonstrating that these cells are Bergmann glia. In contrast, GFP was not expressed in any

calbindin-positive Purkinje neurons (Fig. 2F). In the granule cell layer, GFP was expressed in stellate-shaped astrocytes that were positive for both GFAP and S100 (*data not shown*). In addition, a small portion (7.2%, n=3 mice) of NeuN-positive granule cells expressed GFP (Fig. 2D), which is consistent with the recent report that some progenitors that give rise to postnatally born granule cells can express GFAP (Lee et al. 2005; Schuller et al. 2008; Silbereis et al. 2010). Parvalbumin-positive basket/stellate cells did not express GFP (Fig. 2E). Together, these findings show that in the cerebellar cortex of these transgenic mice, Cre-recombinase activity is targeted selectively to essentially all Bergmann glia and to no Purkinje or basket cells, to most stellate astrocytes and to a small sub-population (about 7%) of granule neurons.

Bergmann glial fibers degenerated during late postnatal development in APC-CKO mice

Since cerebellar cortex was the major site of degeneration in APC-CKO mice, and since Bergmann glia are the major cell type targeted in the cerebellar cortex of this mouse model, we next examined whether Bergmann glia were affected by APC deletion. At P3 in control mice, GFAP was barely detectable, whereas the expression of Nestin, a marker for embryonic radial glia, was still observed in Bergmann glia. The morphology and distribution of Nestin-positive Bergmann glia were indistinguishable between APC-CKO and control mice (Fig. 3A, B), indicating that the early development of Bergmann glia proceeded normally in APC-CKO mice. At P10 in control mice, GFAP expression was robust in Bergmann glia and GFAP-positive radial fibers spanned the entire molecular layer to the pial surface in a manner similar to that observed at P21 and in adult mice (Fig. 3C, E). This observation is consistent with the notion that GFAP expression in Bergmann glia is elevated during the first postnatal week (Landry et al. 1990; Weir et al. 1984). At P10 in APC-CKO mice, the radial scaffold of GFAP-positive fibers was maintained, but the density of fibers began to decrease slightly in lobules VI, VII, VIII (Fig. 3D). Importantly, at P21 in APC-CKO mice, Bergmann glial fibers were markedly disorganized, so that radial fibers spanning the molecular layer had mostly disappeared in the severely affected regions, and stellate-shaped GFAP-positive cells were present in the molecular layer (Fig. 3F). In marked contrast, astrocytes in the granule cell layer, the cerebellar white matter, and the pons displayed no identifiable changes in their distribution and morphology (Fig. 3G–L). These findings indicate an essential role for APC in maintaining the unique morphology of Bergmann glia as compared with other cerebellar astroglia.

Abnormal translocation of Bergmann glia into the molecular layer in APC-CKO mice

The degeneration of radial glial fibers might be attributed either to non-lethal morphological changes or to the outright cell death of Bergmann glia. To differentiate these possibilities, we first analyzed and quantified the number of S100-positive glia in both the Purkinje cell and molecular layers. In control mice at P21, the vast majority of S100-positive cells were located in the Purkinje cell layer and only a few cells were identified in the molecular layer. Thus, most of S100-positive cells in these regions are likely to be Bergmann glia. In CKO mice at the same age, the number of S100-positive cells was significantly decreased in the Purkinje cell layer compared to that in control mice (47% of controls). However, the number of S100-positive cells was markedly and significantly increased in the molecular layer (7-fold increase, Fig. 4A, B) and the number of cells positive for other Bergmann glial markers BLBP and Sox9 similarly increased in the molecular layer of APC-CKO mice (Fig. 4A).

To determine whether Bergmann glia were undergoing cell death, we next counted the number of cells undergoing apoptosis, as detected by cleaved caspase-3. The number of caspase-3-positive cells was not significantly increased in the entire cerebellar cortex of APC-CKO mice both at P14 and P21. In addition, we found that caspase-3-positive cells were mostly negative for S100 in the Purkinje cell and molecular layers of APC-CKO mice

(Fig. 4C). Thus, the death of Bergmann glia is unlikely to play a substantive role in the degeneration of their fibers. This notion is further supported by our finding that the total number of S100-positive cells in the Purkinje cell and molecular layers was not significantly decreased in APC-CKO mice (Fig. 4B). Together, these findings show that in APC-CKO mice the Bergmann glia did not die but translocated from the Purkinje cell layer into the molecular layer.

Progressive accumulation of beta-catenin in APC-deficient Bergmann glia

To study the consequence of APC deletion for the canonical Wnt signaling pathway in Bergmann glia, we examined the distribution and accumulation of beta-catenin in the cerebellar cortex of APC-CKO mice. Beta-catenin-immunoreactivity was barely detectable and indistinguishable between APC-CKO and control mice at P3. Beta-catenin accumulation in the cerebellar cortex of APC-CKO mice became apparent at P10 when the degeneration of radial fibers started. The majority of beta-catenin-accumulated cells were located in the Purkinje cell layer at this time point although a few were also observed in the molecular and granule cell layers. At P21, beta-catenin accumulated cells were broadly distributed in the molecular layer, whereas the number of them was either unchanged or decreased in the granule cell layer and the Purkinje cell layer, respectively (Fig. 5A). Beta-catenin-accumulated cells in the Purkinje cell and molecular layers were positive for GFAP and S100 but negative for calbindin (Fig. 5B, C). Although APC should be deleted in a portion (7%) of granule cells as well, no beta-catenin accumulation was identified in NeuN-positive granule cells or Pax6-positive migrating granule cells (Fig. 5C). Thus, these findings show that beta-catenin was accumulated selectively in Bergmann glia during the period of their translocation into the molecular layer.

Morphological transformation of Bergmann glia into stellate-shaped astroglia

We next analyzed the detailed morphological changes of APC-deficient Bergmann glia during the late postnatal period. At P14, the majority of Bergmann glia still remained in the Purkinje cell layer and the radial fibers spanned the entire molecular layer (Fig. 6A). Nevertheless, a significant portion of Bergmann glia began to translocate into the molecular layer at this time point. Intriguingly, these cells still maintained radial glia morphology. Their radial fibers became shorter but still reached the pial surface and made contacts with the basement membrane (Fig. 6B, C). Thus, the translocation of Bergmann glia into the molecular layer preceded a loss of their pial contact. In addition to becoming shorter, the radial fibers of APC-deficient Bergmann glia were thick and smooth-surfaced, and fine collateral branches of the radial fibers that filled the molecular layer markedly decreased (Fig. 6E) compared to those of controls (Fig. 6D). These affected Bergmann glia accumulated beta-catenin (Fig. 6F). At P21, Bergmann glia in the molecular layer lost their radial glia morphology and became hypertrophic with short processes (Fig. 6G, H). They occasionally extended thick processes to make contacts with blood vessels (Fig. 6I) and their morphological features were similar to those of reactive astrocytes.

Taken together, these findings indicate that APC deletion leads to shortening and thickening of Bergmann glial fibers, with a marked reduction of fine branches followed by a loss of their pial contact and the transformation into reactive astrocyte-like cells.

Regional specificity of morphological changes and beta-catenin accumulation

Our results so far demonstrate that loss of APC leads to the accumulation of beta-catenin and the degeneration of radial fibers in Bergmann glia. Since APC should be deleted in not only Bergmann glia but also the entire GFAP-expressing astroglial population in the CNS, we analyzed the morphology and beta-catenin accumulation in other regions. Beta-catenin accumulated cells were also distributed in the granule cell layer and were positive for S100

(Fig. 7A, B, C) as well as GFAP (*data not shown*). Thus, astrocytes in the cerebellar granule cell layer also accumulated beta-catenin in response to APC deletion but no obvious morphological change was detected. In contrast, no increase in beta-catenin-immunoreactivity was identified in the pons (Fig. 7A, B). Despite the broad distribution of the reporter GFP and GFAP-positive astrocytes in the pons of CKO reporter mice, they exhibited neither identifiable morphological change nor beta-catenin accumulation (Fig. 7D, E). We then examined if radial glia morphology is especially vulnerable to APC deletion. Besides cerebellar Bergmann glia, the CNS contains several types of GFAP-expressing cells with a radial morphology such as tanycytes in the hypothalamus and radial astrocytes in the white matter of the spinal cord. Both cell types expressed the reporter GFP and GFAP in CKO reporter mice, but their radial morphology was well preserved. Beta-catenin was apically concentrated in the tanycytes and was barely expressed in the radial astrocytes, which is indistinguishable from those in controls. (Fig. 7F, G). We also studied the expression of *Axin-2* mRNA, a transcriptional target of beta-catenin (Jho et al. 2002), in different regions of APC-CKO and control brains. The expression of *Axin-2* mRNA was significantly higher in the cerebellum, but not significantly different in the pons and the cerebral cortex of APC-CKO mice compared to those of controls (Fig. 7H), which was well correlated with the distribution of beta-catenin. Taken together, these findings show that the effects of APC deletion on beta-catenin accumulation, activation of its target gene and on cell morphology exhibited both cell type and regional specificity among GFAP-positive astroglia.

Ectopic granule cells in APC-CKO mice

We next examined how the degeneration of the Bergmann glial scaffold affected the organization of the cerebellar cortex. At P10, the thickness of the external granule cell layer and the number of migrating $NeuN^+$ granule cells are indistinguishable between control and APC-CKO mice (Fig. 8A). However, at P21, although the thicknesses of the molecular layer, the Purkinje cell layer, and the granule cell layer were indistinguishable between CKO and control mice (Fig. 8A), there was an increased number of NeuN-positive cells in the molecular layer (Fig. 8A) in addition to the translocated Bergmann glia shown above. Some of these NeuN-positive neurons occasionally formed small aggregates beneath the pial surface, but others were separately distributed within the molecular layer. These cells are likely to be ectopic granule cells since NeuN is shown to specifically label granule cells in the cerebellar cortex (Weyer and Schilling 2003). In support of this notion, we observed no difference in the number of parvalbumin-positive basket/stellate cells between CKO and control mice (*data not shown*). Since it was possible that APC was deleted in a portion of granule cells and disturbed their migration, we analyzed the expression of the reporter GFP in the molecular layer of CKO reporter mice. Almost none of the NeuN-positive granule neurons was positive for GFP (Fig. 8B), indicating that their migration was disturbed by a cell non-autonomous mechanism. It is therefore likely that the degeneration of the Bergmann glial scaffold caused ectopic granule cells. Interestingly, we found almost no GFP-positive neurons in the granule cell layer of CKO reporter mice as well (Fig. 8B). This suggests that APC deletion disturbs the differentiation and/or survival of granule cells derived from GFAP-expressing progenitors, which is consistent with our previous finding that APC is critical for the function of GFAP-positive postnatal and adult progenitors (Imura et al. 2010). The importance of the Bergmann glial scaffold as the railway of migrating granule cells has been well documented. The small number of ectopic granule neurons in the molecular layer of APC-CKO mice and their distribution in the molecular layer rather than forming clusters in the proximity of the pial surface, suggested that they had exited the external granule cell layer but failed to reach their normal destination. These observations are consistent with the atrophy of Bergmann glial fibers and a loss of their pial contact that occurred well after the peak of granule cell migration (Fujita 1967).

Degeneration and loss of Purkinje neurons in APC-CKO mice

Lastly, we investigated whether the degeneration of the Bergmann glial scaffold affected the survival of Purkinje neurons. At P21, when the Bergmann glial scaffold was already fully disrupted in APC-CKO mice, the number and dendritic arborization of Purkinje neurons were indistinguishable between CKO and control mice (Fig. 9A, C). By P180, the number of Purkinje neurons was significantly fewer in CKO mice as compared to age-matched littermate controls (Fig. 9B). Purkinje cell loss was particularly severe in lobules VI, VII, and VIII where the degeneration of the Bergmann glial scaffold was most notable. Calbindin-immunoreactivity was markedly decreased in the somata and dendrites of the remaining Purkinje cells (Fig. 9C). In addition, a number of microglial cells had invaded the cerebellar cortex by this age (P180), whereas the distribution of GFAP-positive glia was similar to younger age (Fig. 9D). These findings show that the degeneration of Bergmann glia leads to a pronounced loss of Purkinje neurons and microglial activation by middle age.

Discussion

In the present study, we studied the effects of APC deletion in GFAP-expressing astroglia and demonstrate that 1) APC is required to maintain the unique cellular architecture of Bergmann glia; 2) APC deletion induces the accumulation of beta-catenin in combination with morphological changes in cerebellar Bergmann glia but not in other CNS astroglia; 3) disruption of the normal Bergmann glial scaffold leads to the cell non-autonomous neurodegeneration of Purkinje neurons.

Methodological considerations

Previous studies have demonstrated that the mGFAP-Cre line 73.12 used in this study targets Cre activity selectively to the vast majority of astroglia (and not to other types of glia) in the forebrain and spinal cord and also to certain postnatal GFAP-expressing neural progenitors that generate small subpopulations of neurons in the hippocampus and olfactory bulb (Garcia et al. 2004; Herrmann et al. 2008). For the present study, we conducted a detailed analysis at the single cell level of the targeting of Cre activity in the cerebellum of mGFAP-Cre mice of line 73.12 by using Cre-reporter mice. The overwhelming majority of cells exhibiting Cre-reporter activity were Bergmann glia and astrocytes. In addition a minor population (about 7%) of granule cells was targeted by Cre-mediated recombination, which is consistent with the recent reports showing the existence of small numbers of GFAP-expressing postnatal neural progenitors in this region (Lee et al. 2005; Schuller et al. 2008; Silbereis et al. 2010). Nevertheless, APC-CKO reporter mice also showed that almost all of these APC-deficient granule cells disappeared before the late postnatal period, which is likely to be due to the impaired differentiation and survival of neurons derived from APC-deficient postnatal neural progenitors as we have recently reported (Imura et al. 2010). It is unlikely that the profound changes in the Purkinje cell and molecular layers of the cerebellar cortex in our APC-CKO mice were somehow due to the small and transient population of APC-deficient granule neurons. We therefore conclude that the changes in the cerebellar cortex of APC-CKO mice can be attributed to the loss of APC in Bergmann glia. Regarding astroglia, including Bergmann glia, no definite difference in the proportion of the reporter-positive cells was observed between control and APC-CKO brains, indicating that APC-deficient astroglia are generated and survive.

Roles of APC in Bergmann glia

One main finding of the present study is that APC deletion in Bergmann glia led to the loss of their unique cellular architecture and radial scaffold structure. The contact with the pial basement membrane is an important feature of the Bergmann glial scaffold, and loss of this contact is implicated in the degeneration of Bergmann glial fibers in some genetically

modified mouse models (Belvindrah et al. 2006; Lin et al. 2009). On the other hand, APC-deficient Bergmann glia maintained their radial morphology as well as the contract with the pial surface during the early phase of their changes in cellular structure while their radial fibers shortened and thickened with reduced collateral branching. Thus, the major role of APC in Bergmann glia is likely to be the maintenance of their thin long fibers as well as the projection of fine braches. The molecular mechanism underlying these effects awaits further investigation. The regulation of the microtubule and actin cytoskeletons is the most likely candidate for the action of APC in Bergmann glia (Li et al. 2003; Lippman et al. 2008; Yokota et al. 2009), but the involvement of a beta-catenin-dependent pathway also remains possible. Since beta-catenin not only activates the transcription of its target genes but also regulates the actin cytoskeleton by forming adherens junctions together with cadherins (McCrea et al. 1991), these two pathways could cooperate to maintain the Bergmann glial morphology. Our findings also show that the loss of APC not only resulted in the loss of the typical cellular architecture of Bergmann glia, but that the cells did not die and instead became more astrocyte-like in appearance. In contrast, the morphology of APC-deficient astrocytes was not detectably altered. These observations suggest a fundamental role for APC in maintaining the unique architecture of Bergmann glia that differentiates them from astrocytes.

Regional differences in the changes of APC-deficient astroglia

Although APC will have been deleted in GFAP-positive astroglia broadly distributed throughout the CNS in our model, we found neither detectable morphological changes nor beta-catenin accumulation in astroglia outside the cerebellum. The radial morphology of both hypothalamic tanycytes and spinal cord radial astrocytes was well maintained. One possible explanation for these region and/or cell-type specific effects of APC deletion is an intrinsic property of Bergmann glia. Bergmann glia display a unique morphology that extends numerous collaterals from its radial fibers to ensheath synapses and these branches are highly motile and plastic (Iino et al. 2001; Lippman et al. 2008; Yamada et al. 2000). A requirement for APC may be high in regulating such morphological complexity of Bergmann glia especially during postnatal development. Alternatively, the effects of APC deletion could be determined in a region-specific manner. Wnts are expressed and the Wnt/beta-catenin pathway is active in the postnatal cerebellar cortex, which is implicated in synaptogenesis, dendritogenesis, and angiogenesis (Daneman et al. 2009; Lucas and Salinas 1997; Salinas et al. 1994; Stenman et al. 2008) *add ref*. It is possible that Wnts are also involved in the morphological maturation of Bergmann glia and APC deletion disrupts it. Lastly, it deserves emphasis that the enormous variability in the effects of APC deletion on beta-catenin accumulation, activation of its target gene and on cell morphology among different CNS astroglia not only provides further evidence of the heterogeneity of these cells at both the regional and local level, but also provides evidence for one of the no doubt many molecular mechanisms that may underlie such heterogeneity.

Cell non-autonomous neurodegeneration of Purkinje neurons due to APC-deficient Bergman glia

A second main finding of the present study is that APC-CKO mice exhibited significant cell non-autonomous degeneration of Purkinje neurons, cerebellar cortical atrophy, and signs of motor ataxia by middle age (P180) secondary to APC deficiency in Bergmann glia that resulted in the loss of their normal cellular architecture in late postnatal development. Our single cell histological evaluations clearly demonstrated that Cre activity and APC deletion were targeted selectively to essentially all Bergmann glia and to no Purkinje neurons. The number and morphology of Purkinje cells appeared normal in juvenile mice at P21, by which time there was substantive disruption of the Bergmann glial scaffold. Nevertheless, there was no obvious atrophy of the cerebellar molecular layer at P56. Together, these

observations suggest that the short-term survival and dendritic arborization of Purkinje neurons were relatively well maintained but that their long-term survival was compromised without the normal Bergmann glial scaffold. Identification of the precise mechanisms by which Purkinje neurons degenerate secondary to changes in APC-deficient Bergman glia will require further investigation. Since the collateral branches of Bergmann glial fibers ensheath excitatory synapses on Purkinje cell dendrites to control glutamate clearance, one possibility to explore is that loss of the glial coverage could elicit excitotoxic injury to Purkinje cells. Such non-cell autonomous Purkinje neuron degeneration has been assumed to be responsible in several neurodegenerative disorders such as SCA1 and SCA7 (Custer et al. 2006; Shiwaku et al. 2010). Whether or not dysfunction of APC-related mechanisms plays a role in specific neurological disorders of the cerebellum will also require further investigation. Nevertheless, our results provide direct evidence that cell non-autonomous degeneration of Purkinje neurons in adults can be caused by abnormalities of Bergmann glia that appear in late postnatal development.

Acknowledgments

This work was supported by grants-in-aid from the Ministry of Education, Culture, Sports, Science and Technology of Japan (18500245), research grants from the Foundation for Biomedical Research and Innovation, fellowships from the Rotary Yoneyama Memorial Foundation (X.W.), and National Institutes of Health USA, NINDS NS057624 (M.V.S).

References

Aoki K, Taketo MM. Adenomatous polyposis coli (APC): a multi-functional tumor suppressor gene. J Cell Sci. 2007; 120(Pt 19):3327–35. [PubMed: 17881494]

Belvindrah R, Nalbant P, Ding S, Wu C, Bokoch GM, Muller U. Integrin-linked kinase regulates Bergmann glial differentiation during cerebellar development. Mol Cell Neurosci. 2006; 33(2):109–25. [PubMed: 16914328]

Bhat RV, Baraban JM, Johnson RC, Eipper BA, Mains RE. High levels of expression of the tumor suppressor gene APC during development of the rat central nervous system. J Neurosci. 1994; 14(5 Pt 2):3059–71. [PubMed: 8182459]

Christopherson KS, Ullian EM, Stokes CC, Mullowney CE, Hell JW, Agah A, Lawler J, Mosher DF, Bornstein P, Barres BA. Thrombospondins are astrocyte-secreted proteins that promote CNS synaptogenesis. Cell. 2005; 120(3):421–33. [PubMed: 15707899]

Custer SK, Garden GA, Gill N, Rueb U, Libby RT, Schultz C, Guyenet SJ, Deller T, Westrum LE, Sopher BL, et al. Bergmann glia expression of polyglutamine-expanded ataxin-7 produces neurodegeneration by impairing glutamate transport. Nat Neurosci. 2006; 9(10):1302–11. [PubMed: 16936724]

Daneman R, Agalliu D, Zhou L, Kuhnert F, Kuo CJ, Barres BA. Wnt/beta-catenin signaling is required for CNS, but not non-CNS, angiogenesis. Proc Natl Acad Sci U S A. 2009; 106(2):641–6. [PubMed: 19129494]

Eiraku M, Tohgo A, Ono K, Kaneko M, Fujishima K, Hirano T, Kengaku M. DNER acts as a neuron-specific Notch ligand during Bergmann glial development. Nat Neurosci. 2005; 8(7):873–80. [PubMed: 15965470]

Fujita S. Quantitative analysis of cell proliferation and differentiation in the cortex of the postnatal mouse cerebellum. J Cell Biol. 1967; 32(2):277–87. [PubMed: 10976221]

Garcia AD, Doan NB, Imura T, Bush TG, Sofroniew MV. GFAP-expressing progenitors are the principal source of constitutive neurogenesis in adult mouse forebrain. Nat Neurosci. 2004; 7(11): 1233–41. [PubMed: 15494728]

Grosche J, Matyash V, Moller T, Verkhratsky A, Reichenbach A, Kettenmann H. Microdomains for neuron-glia interaction: parallel fiber signaling to Bergmann glial cells. Nat Neurosci. 1999; 2(2): 139–43. [PubMed: 10195197]

Hanson CA, Miller JR. Non-traditional roles for the Adenomatous Polyposis Coli (APC) tumor suppressor protein. Gene. 2005; 361:1–12. [PubMed: 16185824]

Herrmann JE, Imura T, Song B, Qi J, Ao Y, Nguyen TK, Korsak RA, Takeda K, Akira S, Sofroniew MV. STAT3 is a critical regulator of astrogliosis and scar formation after spinal cord injury. J Neurosci. 2008; 28(28):7231–43. [PubMed: 18614693]

Iino M, Goto K, Kakegawa W, Okado H, Sudo M, Ishiuchi S, Miwa A, Takayasu Y, Saito I, Tsuzuki K, et al. Glia-synapse interaction through Ca2+-permeable AMPA receptors in Bergmann glia. Science. 2001; 292(5518):926–9. [PubMed: 11340205]

Imura T, Tane K, Toyoda N, Fushiki S. Endothelial cell-derived bone morphogenetic proteins regulate glial differentiation of cortical progenitors. Eur J Neurosci. 2008; 27(7):1596–606. [PubMed: 18380662]

Imura T, Wang X, Noda T, Sofroniew MV, Fushiki S. Adenomatous polyposis coli is essential for both neuronal differentiation and maintenance of adult neural stem cells in subventricular zone and hippocampus. Stem Cells. 2010 in press.

Ivaniutsin U, Chen Y, Mason JO, Price DJ, Pratt T. Adenomatous polyposis coli is required for early events in the normal growth and differentiation of the developing cerebral cortex. Neural Develop. 2009; 4(1):3.

Jho EH, Zhang T, Domon C, Joo CK, Freund JN, Costantini F. Wnt/beta-catenin/Tcf signaling induces the transcription of Axin2, a negative regulator of the signaling pathway. Mol Cell Biol. 2002; 22(4):1172–83. [PubMed: 11809808]

Kawamoto S, Niwa H, Tashiro F, Sano S, Kondoh G, Takeda J, Tabayashi K, Miyazaki J. A novel reporter mouse strain that expresses enhanced green fluorescent protein upon Cre-mediated recombination. FEBS Lett. 2000; 470(3):263–8. [PubMed: 10745079]

Kinzler KW, Nilbert MC, Su LK, Vogelstein B, Bryan TM, Levy DB, Smith KJ, Preisinger AC, Hedge P, McKechnie D, et al. Identification of FAP locus genes from chromosome 5q21. Science. 1991; 253(5020):661–5. [PubMed: 1651562]

Landry CF, Ivy GO, Brown IR. Developmental expression of glial fibrillary acidic protein mRNA in the rat brain analyzed by in situ hybridization. J Neurosci Res. 1990; 25(2):194–203. [PubMed: 2319628]

Lee A, Kessler JD, Read TA, Kaiser C, Corbeil D, Huttner WB, Johnson JE, Wechsler-Reya RJ. Isolation of neural stem cells from the postnatal cerebellum. Nat Neurosci. 2005; 8(6):723–9. [PubMed: 15908947]

Li H, Berlin Y, Hart RP, Grumet M. Microtubules are critical for radial glial morphology: possible regulation by MAPs and MARKs. Glia. 2003; 44(1):37–46. [PubMed: 12951655]

Lin Y, Chen L, Lin C, Luo Y, Tsai RY, Wang F. Neuron-derived FGF9 is essential for scaffold formation of Bergmann radial fibers and migration of granule neurons in the cerebellum. Dev Biol. 2009; 329(1):44–54. [PubMed: 19232523]

Lippman JJ, Lordkipanidze T, Buell ME, Yoon SO, Dunaevsky A. Morphogenesis and regulation of Bergmann glial processes during Purkinje cell dendritic spine ensheathment and synaptogenesis. Glia. 2008; 56(13):1463–77. [PubMed: 18615636]

Lucas FR, Salinas PC. WNT-7a induces axonal remodeling and increases synapsin I levels in cerebellar neurons. Dev Biol. 1997; 192(1):31–44. [PubMed: 9405095]

McCrea PD, Turck CW, Gumbiner B. A homolog of the armadillo protein in Drosophila (plakoglobin) associated with E-cadherin. Science. 1991; 254(5036):1359–61. [PubMed: 1962194]

Nathke IS. The adenomatous polyposis coli protein: the Achilles heel of the gut epithelium. Annu Rev Cell Dev Biol. 2004; 20:337–66. [PubMed: 15473844]

Nishisho I, Nakamura Y, Miyoshi Y, Miki Y, Ando H, Horii A, Koyama K, Utsunomiya J, Baba S, Hedge P. Mutations of chromosome 5q21 genes in FAP and colorectal cancer patients. Science. 1991; 253(5020):665–9. [PubMed: 1651563]

Salinas PC, Fletcher C, Copeland NG, Jenkins NA, Nusse R. Maintenance of Wnt-3 expression in Purkinje cells of the mouse cerebellum depends on interactions with granule cells. Development. 1994; 120(5):1277–86. [PubMed: 8026336]

Schuller U, Heine VM, Mao J, Kho AT, Dillon AK, Han YG, Huillard E, Sun T, Ligon AH, Qian Y, et al. Acquisition of granule neuron precursor identity is a critical determinant of progenitor cell

competence to form Shh-induced medulloblastoma. Cancer Cell. 2008; 14(2):123–34. [PubMed: 18691547]

Shibata H, Toyama K, Shioya H, Ito M, Hirota M, Hasegawa S, Matsumoto H, Takano H, Akiyama T, Toyoshima K, et al. Rapid colorectal adenoma formation initiated by conditional targeting of the Apc gene. Science. 1997; 278(5335):120–3. [PubMed: 9311916]

Shiwaku H, Yoshimura N, Tamura T, Sone M, Ogishima S, Watase K, Tagawa K, Okazawa H. Suppression of the novel ER protein Maxer by mutant ataxin-1 in Bergman glia contributes to non-cell-autonomous toxicity. EMBO J. 2010; 29(14):2446–60. [PubMed: 20531390]

Silbereis J, Heintz T, Taylor MM, Ganat Y, Ment LR, Bordey A, Vaccarino F. Astroglial cells in the external granular layer are precursors of cerebellar granule neurons in neonates. Mol Cell Neurosci. 2010; 44(4):362–73. [PubMed: 20470892]

Stenman JM, Rajagopal J, Carroll TJ, Ishibashi M, McMahon J, McMahon AP. Canonical Wnt signaling regulates organ-specific assembly and differentiation of CNS vasculature. Science. 2008; 322(5905):1247–50. [PubMed: 19023080]

Temburni MK, Rosenberg MM, Pathak N, McConnell R, Jacob MH. Neuronal nicotinic synapse assembly requires the adenomatous polyposis coli tumor suppressor protein. J Neurosci. 2004; 24(30):6776–84. [PubMed: 15282282]

Weir MD, Patel AJ, Hunt A, Thomas DG. Developmental changes in the amount of glial fibrillary acidic protein in three regions of the rat brain. Brain Res. 1984; 317(2):147–54. [PubMed: 6148128]

Weyer A, Schilling K. Developmental and cell type-specific expression of the neuronal marker NeuN in the murine cerebellum. J Neurosci Res. 2003; 73(3):400–9. [PubMed: 12868073]

Yamada K, Fukaya M, Shibata T, Kurihara H, Tanaka K, Inoue Y, Watanabe M. Dynamic transformation of Bergmann glial fibers proceeds in correlation with dendritic outgrowth and synapse formation of cerebellar Purkinje cells. J Comp Neurol. 2000; 418(1):106–20. [PubMed: 10701759]

Yokota Y, Kim WY, Chen Y, Wang X, Stanco A, Komuro Y, Snider W, Anton ES, Rusan NM, Akong K, et al. The adenomatous polyposis coli protein is an essential regulator of radial glial polarity and construction of the cerebral cortex. Neuron. 2009; 61(1):42–56. [PubMed: 19146812]

Zerlin M, Goldman JE. Interactions between glial progenitors and blood vessels during early postnatal corticogenesis: blood vessel contact represents an early stage of astrocyte differentiation. J Comp Neurol. 1997; 387(4):537–46. [PubMed: 9373012]

Zhou FQ, Zhou J, Dedhar S, Wu YH, Snider WD. NGF-induced axon growth is mediated by localized inactivation of GSK-3beta and functions of the microtubule plus end binding protein APC. Neuron. 2004; 42(6):897–912. [PubMed: 15207235]

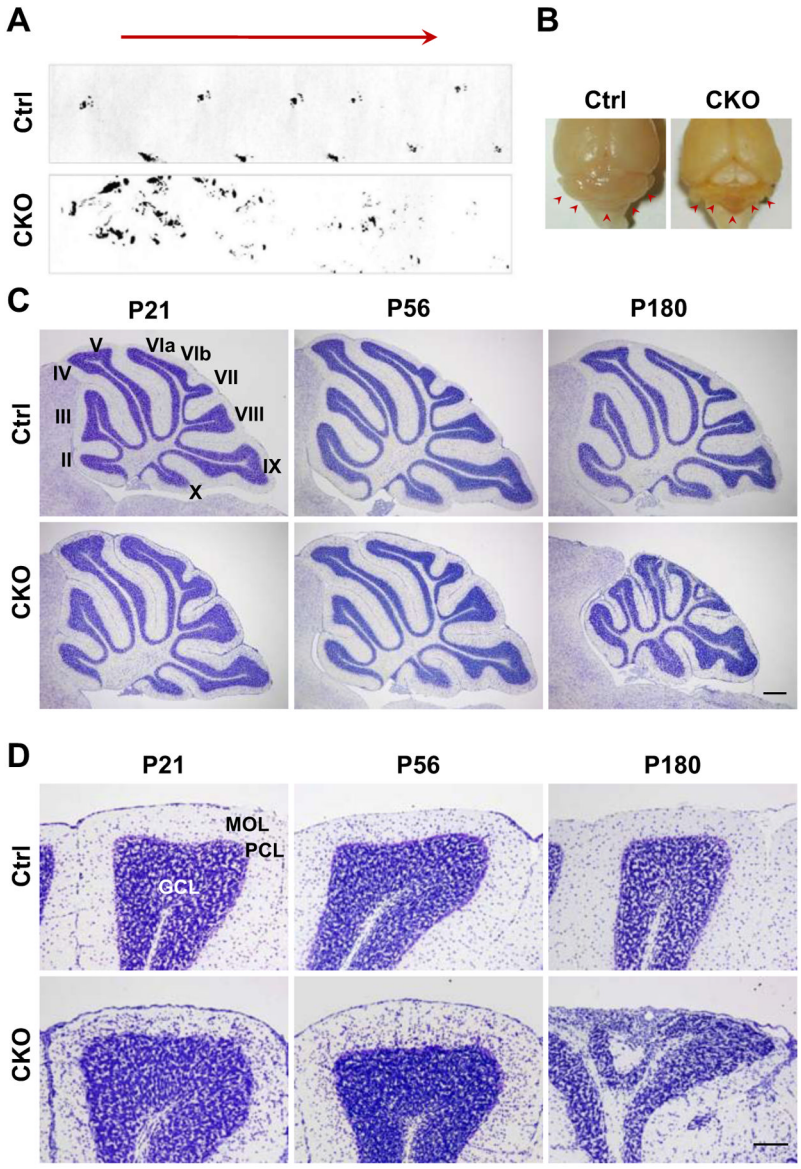

Figure 1.

Motor coordination deficits and cerebellar atrophy of APC-CKO mice by middle age. *A.* The footprint patterns of a middle-aged (P180) CKO mouse and a littermate control (Ctrl). *B.* Macroscopic appearance of middle-aged CKO and Ctrl brains. Note that the cerebellum of CKO mouse is smaller compared to that of Ctrl (*arrowhead*). *C.* Progressive cerebellar atrophy in CKO mice by age. Nissl staining shows that the cerebella of CKO mice at P21 and P56 were normal in size and lobulation, whereas that of CKO mice at P180 exhibits a marked atrophy. *D.* Magnified views of Nissl-stained lobule VIII. The cerebellar cortex of CKO mice at P180 is severely disorganized with a marked reduction in MOL thickness, whereas the cerebellar cytoarchitecture of P21 and P56 CKO mice is indistinguishable from that of Ctrl except for an increased cell density in the MOL. Scale Bar: C, 300 μm; D, 100 μm. P, postnatal day; PCL, Purkinje cell layer; MOL, molecular layer; GCL, granule cell layer.

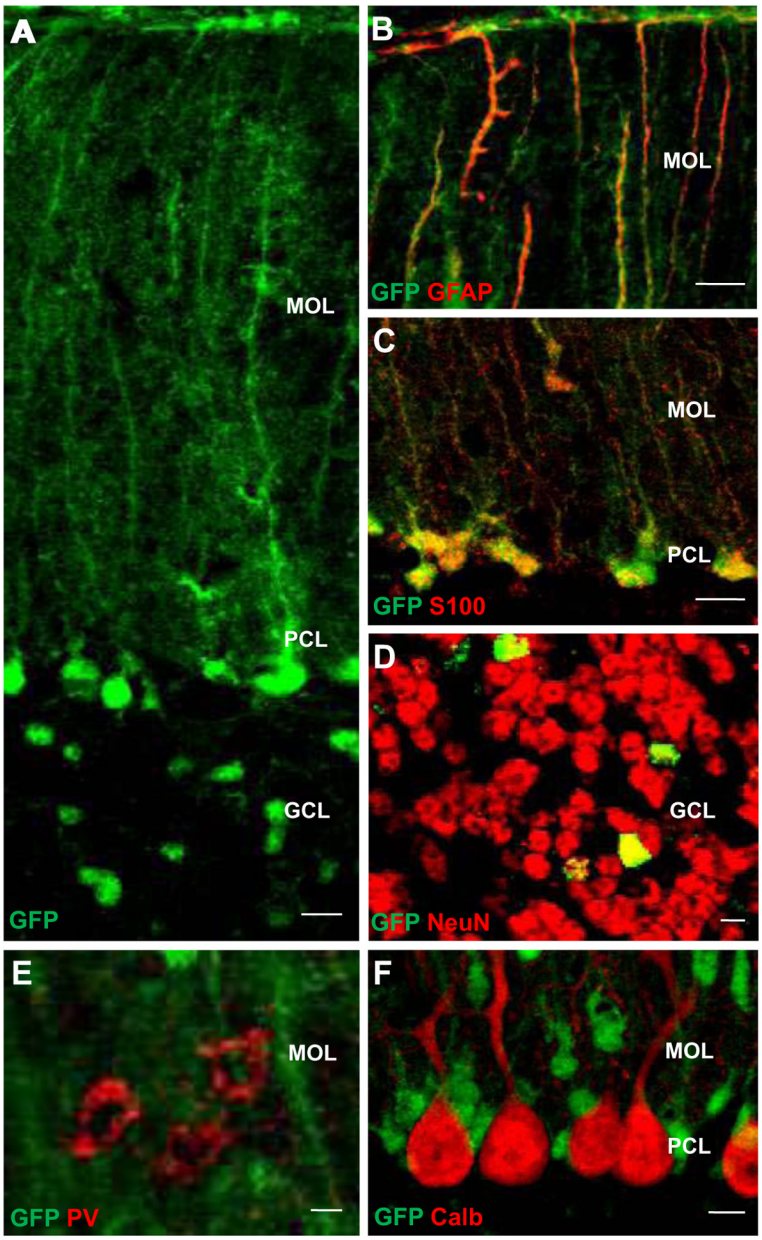

Figure 2.

mGFAP promoter directs Cre activity to Bergmann glia and a small sub-population of granule cells in the cerebellar cortex. The reporter protein GFP is expressed in the cells whose somata are located in the PCL and radial fibers span the entire MOL with numerous collateral branches in adult control mGFAP-Cre reporter mice (*A*). They are positive for both GFAP (*B*) and S100(*C*). A scattered GFP^+ cells are also distributed in the GCL (*A*) and some of them are positive for a granule cell marker NeuN(*D*). No GFP expression is identified in parvalbumin(PV)-positive stellate/basket cells (*E*) and calbindin(Calb)-positive Purkinje cells (*F*). Scale bar: A, B, C, F, 10 μm; D, E, 5 μm. PCL, Purkinje cell layer; MOL, molecular layer; GCL, granule cell layer.

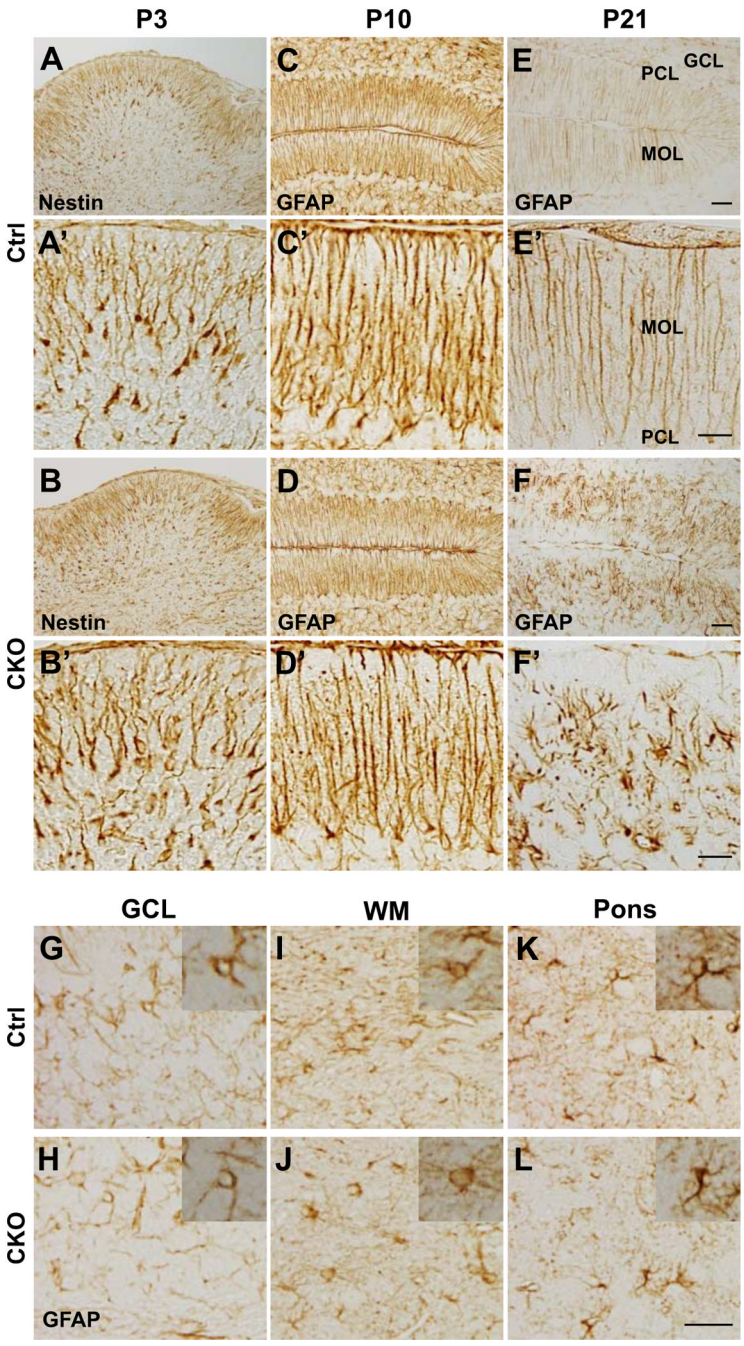

Figure 3.

Degeneration of Bergmann glial fibers in APC-CKO mice during the late postnatal period. Representative images of the cerebellar cortices (A–F) and their magnified views (A′–F′) stained by either Nestin or GFAP in control (Ctrl) and CKO mice at different postnatal ages. At P3, Bergmann glia are positive for an embryonic radial glia marker Nestin and their radial fibers are indistinguishable between Ctrl (*A*) and CKO mice *(B*). At P10, the radial fibers are positive for GFAP and the density of $GFAP^+$ fibers is only slightly decreased in CKO mice (*D*) as compared to that in Ctrl(*C*). At P21, the radial fibers are markedly decreased, whereas stellate-shaped $GFAP^+$ cells are present in the MOL of APC-CKO mice (*F*). In contrast, the distribution and morphology (*inset*) of GFAP-positive astrocytes in the

granule cell layer (*G*, *H*), the cerebellar white matter (*I*, *J*), and the pons (*K*, *L*) are indistinguishable between Ctrl and CKO mice at P21. Scale Bar: 30 μm. P, postnatal day; PCL, Purkinje cell layer; MOL, molecular layer; GCL, granule cell layer; WM, cerebellar white matter.

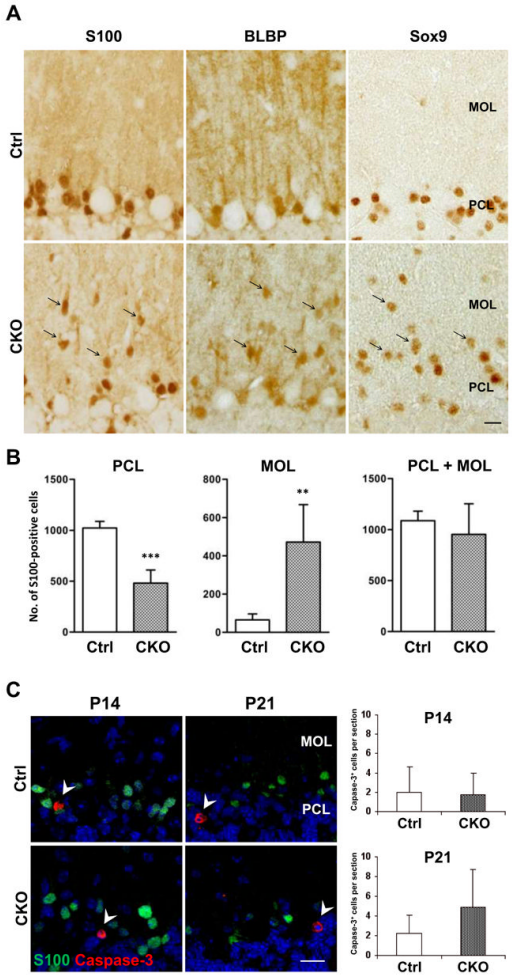

Figure 4.

Translocation of Bergmann glial cell bodies into the MOL in APC-CKO mice. *A.* The cells positive for Bergmann glial markers S100, BLBP, and Sox9 are predominantly localized in the PCL and only a few are found in the MOL of control mice (Ctrl) at P21. In contrast, a number of Bergmann glial markers-positive cells are distributed within the MOL of CKO mice at the same age (*arrow*). *B.* Quantification of $S100^+$ cells in the PCL and MOL. The number of $S100^+$ cells is significantly lower in the PCL but significantly higher in the MOL of CKO mice compared to those of Ctrl, whereas the total number of $S100^+$ cells in the MOL and PCL is not significantly different. n=5, $^{**}p<0.01$, $^{***}p<0.001$ versus controls, *t* test. *C.* No increase in glial cell apoptosis in the cerebellar cortex of CKO mice. Representative images and quantification of caspase-3^+ cells in the cerebellar cortex. The number of caspase-3^+ cells is not significantly different between Ctrl and CKO mice at P14 and P21. n=3–4. Note that caspase-3^+ cells are S100-negative (*arrowhead*). Scale Bar: A, C, 10 μm. P, postnatal day; PCL, Purkinje cell layer; MOL, molecular layer; GCL, granule cell layer.

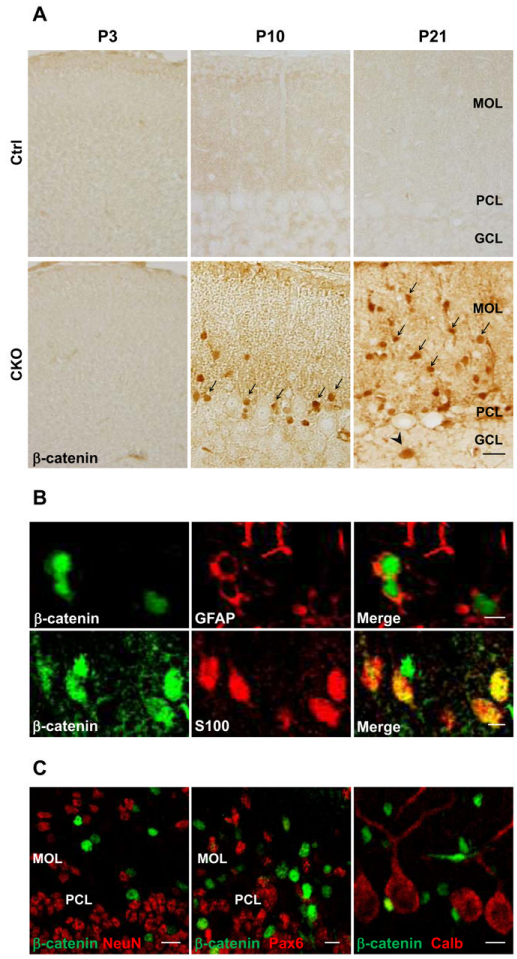

Figure 5.

Progressive accumulation of beta-catenin in Bergmann glia during postnatal development. *A.* Representative images of the cerebellar cortex of control (Ctrl) and APC-CKO mice stained by beta-catenin. No accumulation of beta-catenin is identified in CKO mice at P3. Accumulation of beta-catenin becomes apparent but the vast majority of beta-catenin$^+$ cells are located in the PCL at P10 (*arrow*), whereas many beta-catenin$^+$ cells are distributed within the MOL at P21 (*arrow*). Note that a few beta-catenin$^+$ cells are also identified in the GCL (*arrowhead*). *B.* Double immunofluorescence staining shows that beta-catenin accumulated cells are positive for astroglial markers GFAP and S100. *C.* None of beta-catenin$^+$ cells is positive for a granule cell marker NeuN, an early granule cell progenitor marker Pax6, and a Purkinje cell marker calbindin (Calb). Scale bar: A, 20 μm, B, 5 μm, C, 10 μm. P, postnatal day; PCL, Purkinje cell layer; MOL, molecular layer; GCL, granule cell layer.

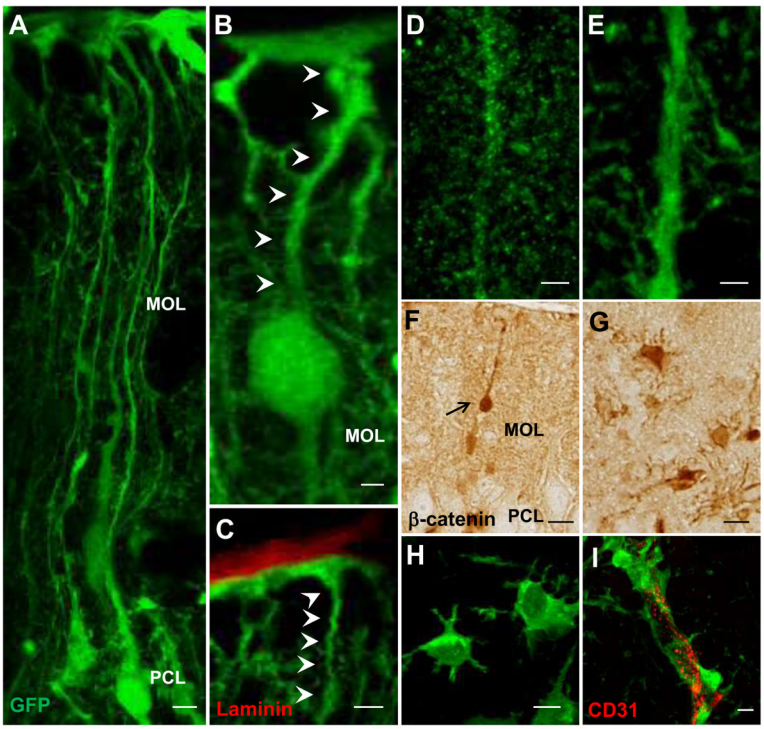

Figure 6.

Morphological transformation of APC-deficient Bergmann glia. Representative images of the reporter GFP-positive cells in the cerebellar cortex of APC-CKO reporter mice. At P14, many GFP-positive Bergmann glia situate in the PCL and their radial fibers span the MOL to the pial surface (*A*). A portion of GFP-positive cells still retain radial glia morphology as well as the contact with the pial surface (*B, C*), but their fibers shorten and the cell bodies translocate into the MOL with beta-catenin accumulation (*B, F*). The radial fibers of APC-deficient Bergmann glia are thick and smooth with a marked reduction of collateral branches (*E*) in comparison to those of control reporter mice (*D*). At P21, the majority of GFP-positive cells loses the pial contact and transforms into a stellate morphology (*G, H*) with the prominent perivascular endfeet (I). Scale bar: A, C, F, G, H, 5μm; B, D, E, I, 2 μm. P, postnatal day; PCL, Purkinje cell layer; MOL, molecular layer; GCL, granule cell layer.

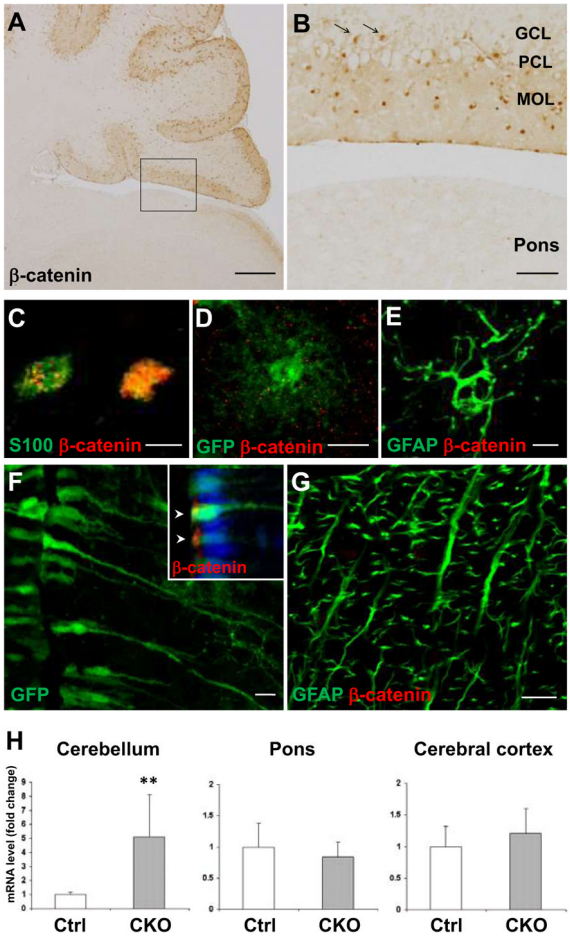

Figure 7.

APC deletion from astroglia induces beta-catenin accumulation and morphological changes in a region-specific manner. Representative images of sagittal sections of APC-CKO mouse brains at P21 stained by beta-catenin (*A*, *B*). *B* shows a magnified image of the boxed area in *A*. In contrast to apparent beta-catenin accumulation in the cerebellar cortex, no increase in beta-catenin immunoreactivity is observed in the pons. Note that beta-catenin$^+$ cells are identified not only in the MOL/PCL but also in the GCL (*arrow in B*). Beta-catenin$^+$ cells in the GCL are positive for an astroglial marker S100 (*C*). The reporter GFP$^+$ and GFAP$^+$ cells are broadly distributed in the pons of CKO reporter mice, but they do not accumulate beta-catenin (*D*, *E*). GFP$^+$ tanycytes in the hypothalamus (*F*) and GFAP$^+$ radial astrocytes in the white matter of the spinal cord (*G*) maintain their radial morphology and show no accumulation of beta-catenin in CKO reporter mice. Note that beta-catenin is apically concentrated (*arrow head*) in GFP$^+$ tanycytes (*inset in F*) but is not accumulated within the nucleus (*blue*). Quantitative RT-PCR analysis shows that the expression of *Axin-2* mRNA significantly increases in the cerebellum, but neither in the pons nor in the cerebral cortex of CKO mice at P21 compared to those of controls (*H*). $^{**}p<0.01$, *t* test. n=4–6. Scale bar: A, 300 μm; B, 50 μm; C, D, E, 5 μm; F, G, 10 μm. P, postnatal day; PCL, Purkinje cell layer; MOL, molecular layer; GCL, granule cell layer.

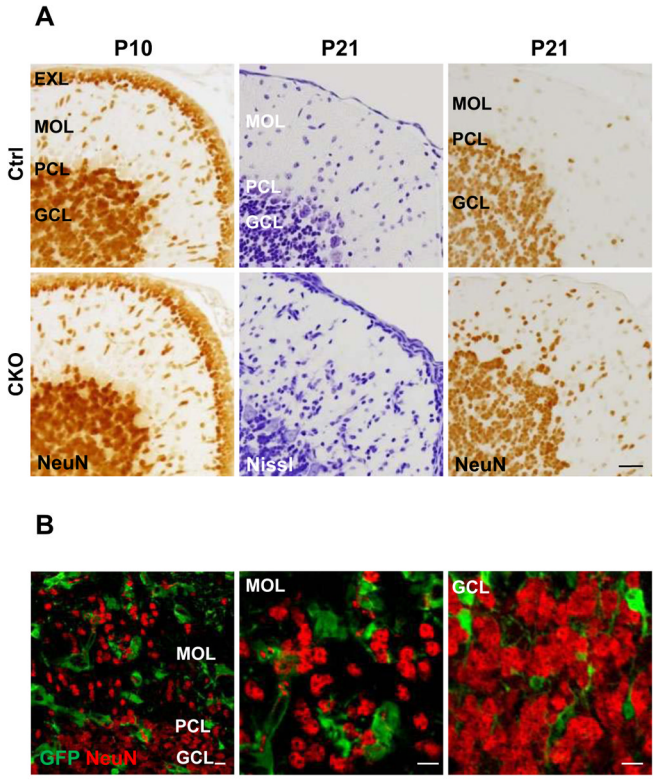

Figure 8.

Ectopic granule cells in the molecular layer of APC-CKO mice. *A.* Representative images of the cerebellar cortices of control (Ctrl) and CKO mice stained by Nissl and a granule cell marker NeuN. The thickness of the EXL and the number of migrating $NeuN^+$ granule cells are indistinguishable between Ctrl and CKO mice at P10. The number of Nissl-stained cells in the MOL increases and a portion of them are positive for NeuN in CKO mice at P21, whereas only a few $NeuN^+$ cells are identified in the MOL of Ctrl at the same age. *B.* Ectopic granule cells in the MOL are negative for GFP in CKO reporter mice at P21 (*left and middle panels*). Note that almost no GFP-positive granule cell is identified in the GCL as well (*right panel*). Scale bar: A, 25 μm; B, 10μm. P, postnatal day; PCL, Purkinje cell layer; MOL, molecular layer; GCL, granule cell layer; EXL, external granule cell layer.

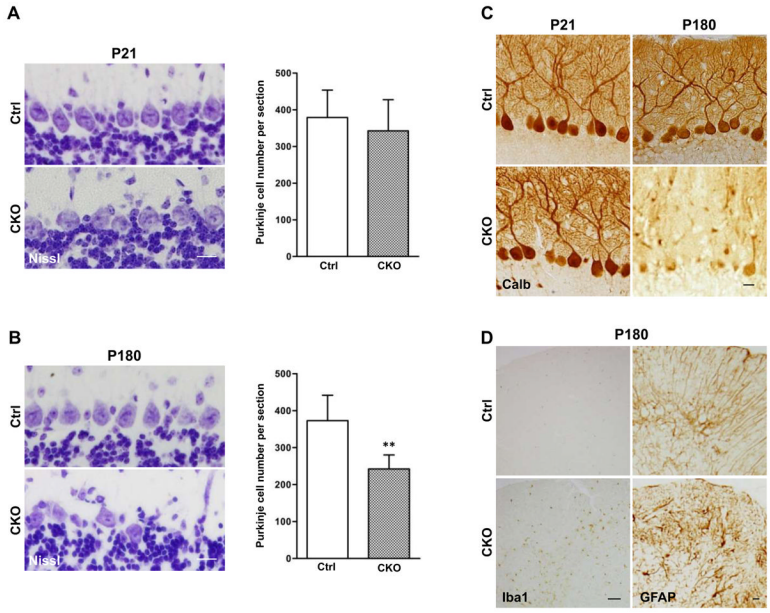

Figure 9.

Cell non-autonomous neurodegeneration of Purkinje neurons and microglial activation in middle-aged APC-CKO mice. *A, B.* Representative images of the PCL of control (Ctrl) and CKO mice stained by Nissl and quantification of Purkinje cell number. At P21, the alignment of Purkinje cells in CKO mice is well preserved and the number is not significantly different (p=0.49). At P180, the loss of Purkinje cells becomes apparent and the number is significantly fewer in CKO mice. n=5, $^{**}p<0.01$ versus controls, *t* test. *C.* Representative images of Purkinje neurons of Ctrl and CKO mice stained by calbindin. At P21, the dendritic arborization of Purkinje neurons in CKO mice is indistinguishable from that in Ctrl. At P180, in addition to a decrease in cell number, calbindin-immunoreactivity was markedly reduced in the remaining Purkinje cells. *D.* Representative images of the cerebellar cortices of Ctrl and CKO mice at P180 stained by Iba1 and GFAP. $Iba1^{+}$ microglial cells are broadly distributed in the cerebellar cortex of middle-aged CKO mice. The distribution of $GFAP^{+}$ astroglia remains unchanged in comparison to younger ages but GFAP-immunoreactivity moderately increases. Scale bar: : A, B, 15 μm; C, 20 μm; D, 50 μm. P, postnatal day; PCL, Purkinje cell layer; MOL, molecular layer; GCL, granule cell layer.